Diffusivity in Alumina Scales Grown on Al-MAX Phases

James L. Smialek
Glenn Research Center, Cleveland, Ohio

NASA STI Program . . . in Profile

Since its founding, NASA has been dedicated to the advancement of aeronautics and space science. The NASA Scientific and Technical Information (STI) program plays a key part in helping NASA maintain this important role.

The NASA STI Program operates under the auspices of the Agency Chief Information Officer. It collects, organizes, provides for archiving, and disseminates NASA's STI. The NASA STI program provides access to the NASA Aeronautics and Space Database and its public interface, the NASA Technical Reports Server, thus providing one of the largest collections of aeronautical and space science STI in the world. Results are published in both non-NASA channels and by NASA in the NASA STI Report Series, which includes the following report types:

- TECHNICAL PUBLICATION. Reports of completed research or a major significant phase of research that present the results of NASA programs and include extensive data or theoretical analysis. Includes compilations of significant scientific and technical data and information deemed to be of continuing reference value. NASA counterpart of peer-reviewed formal professional papers but has less stringent limitations on manuscript length and extent of graphic presentations.

- TECHNICAL MEMORANDUM. Scientific and technical findings that are preliminary or of specialized interest, e.g., quick release reports, working papers, and bibliographies that contain minimal annotation. Does not contain extensive analysis.

- CONTRACTOR REPORT. Scientific and technical findings by NASA-sponsored contractors and grantees.

- CONFERENCE PUBLICATION. Collected papers from scientific and technical conferences, symposia, seminars, or other meetings sponsored or cosponsored by NASA.

- SPECIAL PUBLICATION. Scientific, technical, or historical information from NASA programs, projects, and missions, often concerned with subjects having substantial public interest.

- TECHNICAL TRANSLATION. English-language translations of foreign scientific and technical material pertinent to NASA's mission.

Specialized services also include creating custom thesauri, building customized databases, organizing and publishing research results.

For more information about the NASA STI program, see the following:

- Access the NASA STI program home page at *http://www.sti.nasa.gov*

- E-mail your question to *help@sti.nasa.gov*

- Fax your question to the NASA STI Information Desk at 443–757–5803

- Phone the NASA STI Information Desk at 443–757–5802

- Write to:
  STI Information Desk
  NASA Center for AeroSpace Information
  7115 Standard Drive
  Hanover, MD 21076–1320

NASA/TM—2014-218344

Diffusivity in Alumina Scales Grown on Al-MAX Phases

James L. Smialek
Glenn Research Center, Cleveland, Ohio

National Aeronautics and
Space Administration

Glenn Research Center
Cleveland, Ohio 44135

August 2014

Acknowledgments

Level of Review: This material has been technically reviewed by technical management.

Diffusivity in Alumina Scales Grown on Al-MAX Phases

James L. Smialek
National Aeronautics and Space Administration
Glenn Research Center
Cleveland, Ohio 44135

Abstract

Ti$_3$AlC$_2$, Ti$_2$AlC, and Cr$_2$AlC are oxidation resistant MAX phase compounds distinguished by the formation of protective Al$_2$O$_3$ scales with well controlled kinetics. A modified Wagner treatment was used to obtain interfacial grain boundary diffusivity, $\delta D_{gb,O,int.}$, from scale growth rates and corresponding grain size. It is based on the $p(O_2)^{-1/6}$ dependency of $[V_O^{\circ\circ}]$ and oxygen diffusivity, coupled with the effective diffusion constant for short circuit grain boundary paths. Data from the literature for MAX phases was analyzed accordingly, and $\delta D_{gb,O,int.}$ was found to nearly coincide with the Arrhenius line developed for Zr-doped FeCrAl, where:

$$\delta D_{gb,O,int.} = 1.8 \times 10^{-10} \exp\left(\frac{-375 \text{ kJ}}{RT}\right) \text{m}^3\big/\text{s}$$

Furthermore, this oxidation relation suggests the more general format applicable to bulk samples under ambient conditions:

$$\delta D_{gb,O} = 7.567 \times 10^{-8} \exp\left(\frac{-544 \text{ kJ}}{RT}\right) p_{O_2}^{-1/6} \frac{\text{m}^3}{\text{s} \cdot \text{Pa}^{-1/6}}$$

Data from many other FeCrAl(X) studies were similarly assessed to show general agreement with the relation for $\delta D_{gb,O,int.}$. This analysis reinforces the view that protective alumina scales grow by similar mechanisms for these Al-MAX phases and oxidation resistant FeCrAl alloys.

Introduction

MAX phase compounds represent a unique class of ceramic materials with exceptional strain and damage tolerance, thermal shock resistance, and machinability (Barsoum and El-raghy, 2001). While over 60 compounds have been reported, a much smaller subset claims optimum oxidation resistance at temperatures greater than 1000 °C. These include Ti$_3$AlC$_2$, Ti$_2$AlC, and Cr$_2$AlC, which are the primary compounds reported to develop protective alumina scales (Wang and Zhou, 2003a) (Wang and Zhou, 2003b) (Lee and Park, 2007). These properties and attractive thermal expansion matches with alumina, YSZ, or Ni alloys make alumina-forming MAX phase compounds an interesting option for hybrid high temperature systems (Smialek and Garg, 2014).

As with metallic substrates, alumina scale growth on MAX phases has been identified to be controlled by short circuit grain boundary diffusion, primarily oxygen, whereby scale grain growth can reduce the number of short circuit through-paths and directly slow the rate of scale thickening (X.H. Wang, Li, Chen, and Zhou, 2012) (Tallman, Anasori, and Barsoum, 2013) (Song et al., 2012). Here precise analyses of scale microstructure proved that grain growth leads to subparabolic (cubic or quartic) oxidation kinetics, analogous to prior treatments of alumina scales on metallic substrates, such as FeCrAl(X)-type alloys. Furthermore, estimates of oxygen grain boundary diffusion were obtained from modified Wagner models of scale growth. Here excellent agreement was obtained for Ti$_3$AlC$_2$ and FeCrAl-Y$_2$O$_3$ (Wang et al., 2012) (Clemens et al., 1995), suggesting a commonality of the basic transport, rate-controlling mechanism.

In that regard, another solution to the Wagner integral has been recently proposed (Smialek, et al., 2013) (Smialek, et al., 2014). It takes into account the variation of grain boundary diffusivity across the scale, according to $p(O_2)^{-1/6}$, as shown from bulk permeability studies of polycrystalline alumina which yielded (Wada, Matsudaira, and Kitaoka, 2011):

$$\delta D_{gb,O} = 2.207 \times 10^{-9} \exp\left(\frac{-467 \text{ kJ}}{RT}\right) p_{O_2}^{-1/6} \frac{\text{m}^3}{\text{s} \cdot \text{Pa}^{-1/6}} \tag{1}$$

The conventional form of the Wagner equation (where instantaneous $k_{p,i}$ is given by $2x\, dx/dt$ and x is scale thickness) is then coupled with standard relations for D_{eff}. Although grain growth results in subparabolic overall scale growth rates, the Wagner treatment can still be applied to an instantaneous or differential k_p. Assuming negligible contributions from Al outward diffusion, the following Wagner integral was obtained:

$$k_{p,i} = 2x\frac{dx}{dt} = \int_{p_{O_2},int.}^{p_{O_2},\text{gas}} \frac{2\delta D_{gb,O}}{G_i} d\ln p_{O_2} \tag{2}$$

Here δ is the grain boundary width (~ 1 nm), and $D_{gb,O,int.}$ is oxygen diffusivity at the scale-substrate interface. Integration is performed over the $p(O_2)$ gradient across the scale, where $p(O_2)_{int.}$ refers to the equilibrium oxygen pressure at the scale-metal interface, and $p(O_2)_{gas}$ refers to the external oxygen partial pressure. By substitution of Equation (1), It was further shown that the oxygen grain boundary diffusion product can be given by $\Pi/12$, where Π_i is the oxidation product of the instantaneous parabolic rate constant ($k_{p,i}$) and the corresponding grain diameter at that time (G_i):

$$\Pi_i = k_{p,i}G_i = 12\delta D_{gb,O,int.} \tag{3}$$

(This approach essentially parallels that set forth by Pint, albeit with minor alterations (Pint, 1992) (Pint and Deacon, 2005). By applying this to a large data set (for x and G versus T, t) in the oxidation of FeCrAl(Zr), it was then found that (Smialek et al., 2013):

$$\delta D_{gb,O,int.} = 1.8 \times 10^{-10} \exp\left(\frac{-375 \text{ kJ}}{RT}\right) \text{m}^3/\text{s} \tag{4}$$

or about a factor of 10 to 40x lower than those predicted by Equation (1) for undoped bulk alumina. Note that this value applies to diffusivity at the low $p(O_2)$ interface, which had been shown to be operative over 99% of the scale thickness and well above the diffusivity corresponding to atmospheric conditions (Wada et al., 2011).

This was a reasonable baseline for other FeCrAl alloys as well, to be shown in detail later as a well-characterized alumina-forming system. The purpose of the present work is to assess diffusional control of alumina scale growth on MAX phase compounds using the same treatment. The analysis enabled by Equation (3), resulting from the $p(O_2)^{-1/6}$ dependency of diffusion, leads to more appropriate values of $\delta D_{gb,O}$. Data sets where the time dependence of both scale thickness and grain diameter are given lead to the most accurate results, though estimates of $\delta D_{gb,O}$ were included where only average growth rate and grain diameters were reported.

Results and Discussion

Diffusivity analyses of Ti_3AlC_2 oxidation was performed by Wang et al. (Wang et al., 2012). Both instantaneous k_p (figure 6 in Wang) and grain size were measured for 0 to 20 h oxidation at 1000, 1150, and 1250 °C. Since grain size was given only for 1250 °C (figure 9 in Wang), the initial calculation of $\delta D_{gb,O,int.}$ from Equation (4) was limited to that temperature in Figure 1. The results are seen to be quite

close to the fitted line for FeCrAl(Zr). More commonly, $\delta D^{\times}_{gb,O,int.}$ had been assumed to be constant ($\times$) across alumina scales (Clemens et al., 1995) (Young et al., 2010) (Wang et al., 2012), yielding:

$$k_p = \frac{2\delta D^{\times}_{gb,O}}{G} \Delta \ln p(O_2) \qquad (5)$$

This solution of Equation (2) leads to values that are 1/6 $\Delta\ln[p(O_2)]$ lower than those calculated from Equation (3), (Smialek et al., 2013). Also, $p(O_2)_{eq}$ had been calculated at 1000 to 1400 °C from computational thermodynamic codes by Jacobson and Zhang, 2012, (FactSage (Bale et al., 2009) and Pandat (Chen et al., 2002), , yielding this fitted approximation:

$$P_{O_2,eq} \approx 6.117 \times 10^{15} \exp\left(\frac{-1012\,\text{kJ}}{RT}\right) \text{Pa} \qquad (6)$$

Thus the $\delta D^{\times}_{gb,O}$ values reported in (Wang et al., 2012) were multiplied by 1/6 $\Delta\ln[p(O_2)]$ (a factor ranging from 11.5 at 1000 °C to 7.8 at 1400 °C) to yield the open 'X' symbols in Figure 1. Good agreement is shown with the prior calculation from Equation (3) at 1250 °C as well as with the FeCrAl(Zr) baseline. (Note that this treatment for Ti_3AlC_2 assumes a similar and small role of Al activity in the calculation of $p(O_2)_{eq}$ from K_{eq} for Ti_3AlC_2 and FeCrAl.)

Next, data for Ti_2AlC is considered. The interfacial grain size and continuous weight gain were obtained at 1200 °C for 80 h. From the instantaneous power law exponent, n_i, (Song et al., 2012):

$$x^n = kt \qquad (7)$$

and Equation (2), it can be shown that:

$$k_{p,i} = \frac{2x_i^2}{n_i t_i} \qquad (8)$$

This allows $\delta D_{gb,O,int.}$ to be determined by combining Equations (3) and (8), shown in Figure 1 as the upper 'plus' + symbol. Again there is good agreement with the fitted FeCrAl(Zr) line.

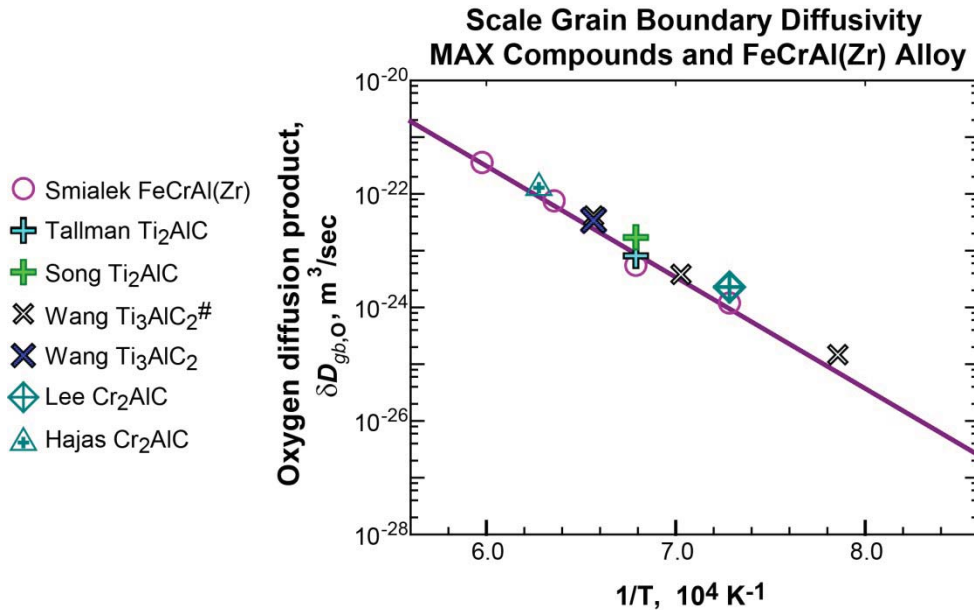Figure 1.—Arrhenius plot of oxygen grain boundary diffusivity estimated for alumina scales grown on Ti_3AlC_2, Ti_2AlC, and Cr_2AlC MAX phase compounds. Results agree with Hoskins 875 FeCrAl(Zr) oxidation behavior within experimental scatter.

Oxidation kinetics and interfacial scale grain size were also measured for Ti_2AlC at 1200 °C for up to 2800 h (Tallman et al., 2013). Relations for subparabolic scale kinetics:

$$x(\mu m) = 1.2(t/t_0)^{0.36} \text{ (h)} \tag{9}$$

and grain growth kinetics:

$$G(\mu m) = 0.295 \times t^{0.31} \text{ (h)} \tag{10}$$

were reported. Equation (9) was used to derive $k_{p,i}$, then combined with Equation (10) to determine $\delta D_{gb,O,int.}$ from Equation (3):

$$\delta D_{gb,O} \text{ (m}^3\text{/s)} = 0.0.254 t^{0.03}\text{(h)} \tag{11}$$

This indicates a very slight time dependence, with $\delta D_{gb,O,int.}$ increasing from 7×10^{-24} to just 9×10^{-24} m^3/s from t=1 to 2800 h. The mid-value of 8.1×10^{-24} m^3/s corresponding to ~100 h is plotted in Figure 1. Again the diffusion product is seen to agree quite well with the FeCrAl(Zr) baseline. TiO$_2$ is often observed to some small degree in Ti-Al-C MAX phase oxidation and may account for the slight offset compared to FeCrAl(Zr).

Finally, the oxidation of Cr_2AlC is addressed. Data for both kinetics and corresponding scale microstructure is sparse. An average parabolic rate constant was reported as 7.5×10^{-11} kg^2/m^{4}s at 1100 °C (50 h). The same authors later present an interfacial microstructure after 480 h oxidation at 1100 °C (Lee 2012). The scale grain size was measured from imprints in the adjacent Cr_7C_3 sublayer as 1.28 ± 0.47 μm. This allows estimates of Π and $\delta D_{gb,O,int.}$, namely 0.10 μm^3/h and 2.28×10^{-24} m^3/s. The latter, shown in Figure 1, is seen to be slightly above the fitted line for FeCrAl(Zr) and within a scatter band typical of the other MAX phase results with similar offsets. Another study examined scales formed on sputter coatings of Cr_2AlC during oxidation at 1230 to 1410 °C for various times (Hajas, et al., 2011). TGA revealed near-parabolic kinetics, and grain structure was revealed by means of FIB-XTEM. Here larger grains are seen to be at the gas-scale interface (scales formed at 1320 °C up to 5 h), at odds with most studies of alumina scales. Nevertheless the rates are reported to be near those obtained for NiAl and bulk Cr_2AlC. A summary of estimated of grain size, Π, and $\delta D_{gb,O,int.}$ is presented in Table 1. Using the longest time and thickest scale as most representative of the average k_p, the obtained diffusion product is seen to agree with the previous data, Figure 1. However, this agreement is subject to questions raised by an uncertain growth direction and by using an average k_p.

TABLE 1.—OXIDATION PRODUCT (Π) AND DIFFUSION PRODUCT ($\delta D_{GB,O}$) FOR Cr_2AlC SPUTTERED FILM. DETERMINED FOR 1320 °C FROM XTEM GRAIN SIZE AND TGA k_P = 3.16×10^{-9} kg^2/m^{4}s (HAJAS, ET AL., 2011)

Time, h	G (fine), μm	G (coarse), μm	Π, μm^3/h	δD_{gb}, m^3/sec	Log δD_{gb}
0.065	?	0.13	0.422	9.765×10^{-24}	−23.010
0.65	0.56	0.71	2.30	5.333×10^{-23}	−22.273
4.7	0.96	1.71	5.55	1.285×10^{-22}	−21.891

Other FeCrAl(X) data. Published FeCrAl(X) oxidation data is often quoted in comparisons of scale grain boundary diffusivity. These are presented in Figure 2 to provide a more global perspective, now all obtained by using Equation (3) in the same framework as above. A few comments are offered below.

A comprehensive study of FeCrAlY oxidation at 1200 °C was presented with detailed microstructural characterizations (Naumenko, Gleeson, Wessel, Singheiser, and Quadakkers, 2007). The precise determination of scale grain size as a function of thickness, coupled with an exact polynomial fit of thickness vs oxidation time, allowed the determination of the unique value for Π = 0.4546 μm^3/h, equivalent to $\delta D_{gb,O,int.}$ = 1.052×10^{-23} m^3/s (Smialek et al., 2013). Because of many overlapping points at 1200 °C, the plot is expanded by alloy group in Figure 3 for clarity. This FeCrAlY datum is quite close to the fitted (dashed) line for FeCrAl(Zr). Grain diameters were not available for the same alloy oxidized in

Scale Grain Boundary Diffusivity
MAX Compounds and FeCrAl(X) Alloys

Legend:
- ○ Smialek FeCrAl(Zr)
- ⊞ Tallman Ti$_2$AlC
- ✚ Song Ti$_2$AlC
- ✖ Wang Ti$_3$AlC$_2$#
- ✖ Wang Ti$_3$AlC$_2$
- ⬖ Lee Cr$_2$AlC
- △ Hajas Cr$_2$AlC
- ⊕ Ramanarayanan FeCrAl(Y$_2$O$_3$)
- ☆ Clemens FeCrAl(Y$_2$O$_3$)#
- ⬡ Tolpygo FeCrAl(Y$_2$O$_3$)
- ⬡ Tolpygo FeCrAl(ZrO$_2$)
- △ Pint FeCrAl
- ▽ Pint FeCrAlY
- □ Naumenko FeCrAlY
- ⊞ Young FeCrAlY#
- ● Messaoudi FeCrAl(Y$_2$O$_3$)
- ● Messaoudi Y-implanted FeCrAl(Zr)
- ● Messaoudi FeCrAl(Zr)

Q=375 +/- 25 kJ/mole

Oxygen diffusion product, δD_{gb},O, m^3/sec
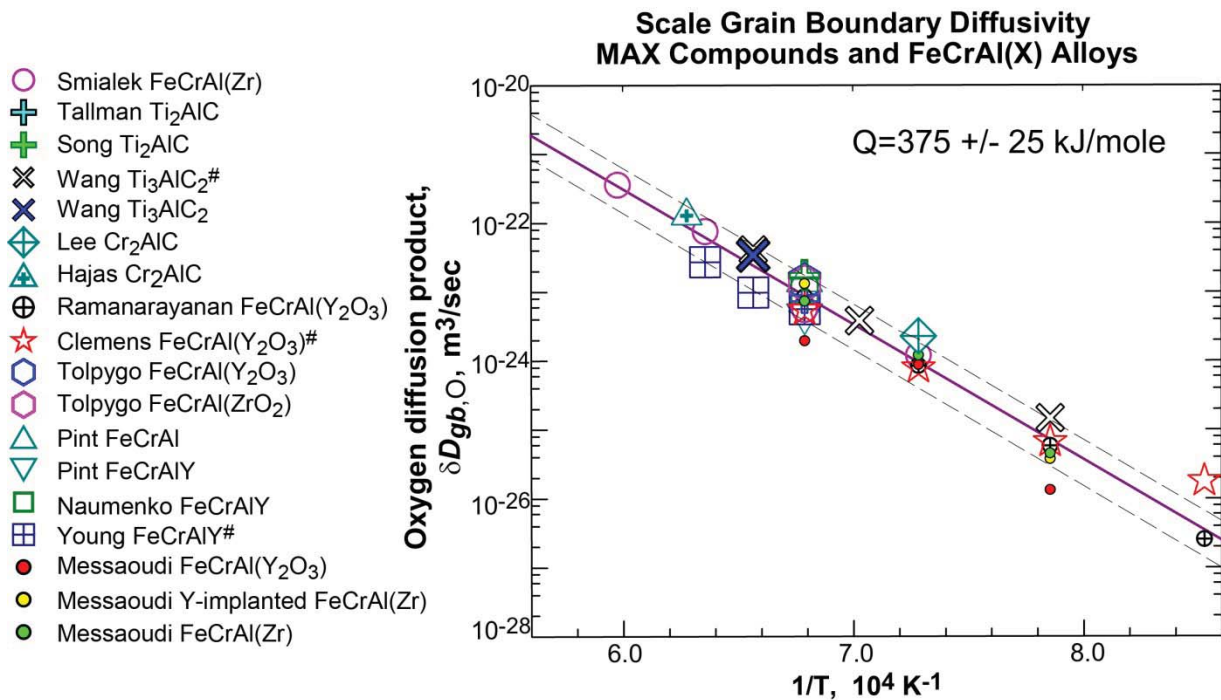
1/T, 10^4 K^{-1}

Figure 2.—Oxygen grain boundary diffusivity from Figure 1 compared to other FeCrAl(X) alloy behavior. Calculated from oxidation data for undoped and Y, Zr, Y$_2$O$_3$, and ZrO$_2$ doped FeCrAl.

Oxygen Grain Boundary Diffusivity in 1200 °C Scales
MAX Phases vs FeCrAl(X)

Legend:
- ✚ Sloof Ti$_2$AlC
- ✚ Tallman Ti$_2$AlC
- ▽ Pint FeCrAl(Y)
- □ Naumenko FeCrAl(Y)
- ⊞ Young FeCrAl(Y)
- ● Messaoudi FeCrAl(Zr)
- ● Smialek FeCrAl(Zr)
- ⊕ Ramanarayanan MA956
- ☆ Clemens MA956
- ● Messaoudi MA 956
- ⬡ Tolpygo MA956
- ⬡ Tolpygo Kanthal APM

Oxygen diffusion product, δD_{gb},O, m^3/sec

Substrate

Ti$_2$AlC, FeCrAl(Y), FeCrAl(Zr), FeCrAl(Y$_2$O$_3$), FeCrAl(ZrO$_2$)
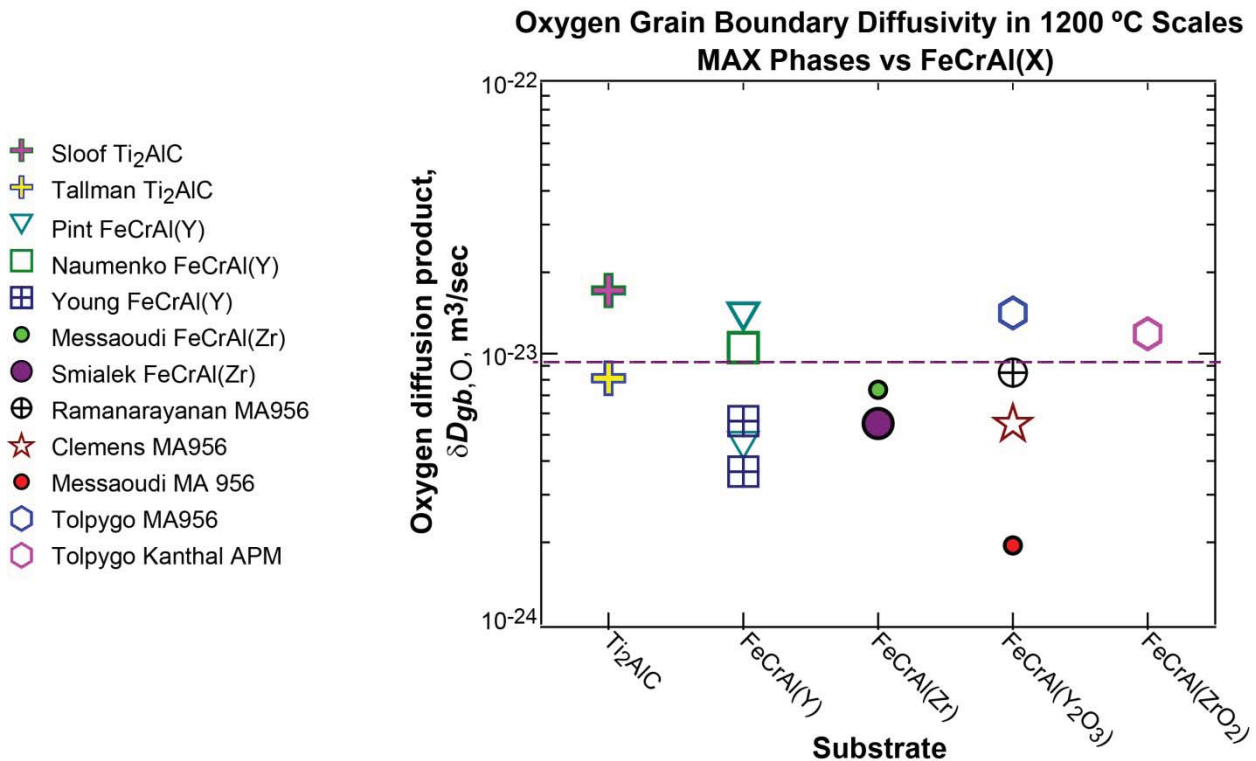
Figure 3.—Expanded 1200 °C diffusivity data from Figure 2 showing overlap and range of variations for specific material classes.

another study using Ar-20% O_2 (Young et al., 2010). However $\delta D^\times_{gb,O}$ data was presented for the Wagner solution assuming constant $\delta D^\times_{gb,O}$ across the interface. As with the Ti_3AlC_2 data, these values were multiplied by the 1/6 $\Delta\ln[p(O_2)]$ correction factor to yield the upper crossed square symbol. The lower symbol corresponds to a similarly corrected value that integrated both variable $\delta D_{gb,O}$ and grain size across the scale thickness (Young et al., 2010). Finally, data for G=0.5 μm scales grown on FeCrAl and FeCrAlY after 100 h at 1200 °C (B. Pint, 1992) are shown as the upper and lower triangles, respectively. They indicate a reduced diffusivity of ~3x due to Y-doping. Values for these FeCrAlY alloys are close and ~2x below the fitted FeCrAl(Zr) line.

Hoskins 875 FeCrAl(Zr) (circles) were used to define our Arrhenius line in Figures 1 and 2. However, the 1200 °C value is shown to be about 40% below the fitted line (Figure 3) for unknown reasons (Smialek et al., 2013). This applies to measurements made on numerous separate samples over a 10, 20, 50, 100, and 200 h time period. By comparison, $\delta D_{gb,O,int.}$ calculated from a single 48 h grain size and fitted k_p for an Imphy FeCrAl(Zr) alloy, similarly doped with 0.2 wt.% Zr, follows the same temperature dependence in Figure 2, as does their Y-implanted FeCrAl(Zr), but with more scatter (Messaoudi, Huntz, and Lesage, 1998).

Next we consider a number of studies of the Y_2O_3 oxide-dispersed MA 956 alloy. In one of the earliest modified Wagner treatments of alumina scales, parabolic kinetics were found from 900 to 1200 °C in 25 to 100 h tests (Ramanarayanan, Raghavan, and Petkovic-Luton, 1984). While some scatter existed, he described the average behavior by one Arrhenius relation:

$$k_p = 1.2\times10^{-2}\exp(-388 \text{ kJ}/RT) \text{ m}^2/\text{s} \tag{12}$$

A slowly changing, temperature independent interfacial grain size of 0.5 μm was reported, with little elaboration. This allows $\delta D_{gb,O, int.}$ to be roughly approximated according to Equation (3) and are shown as the crossed circles quite near the FeCrAl(Zr) baseline in Figures 2 and 3. In a subsequent study, grain boundary diffusivity was determined for MA 956 over the same temperature range assuming a constant $\delta D^\times_{gb,O}$ across the scale (Clemens et al., 1995). Grain size was again reported to be relatively temperature independent, but ranged from 0.2 to 1 μm across the thickness, again with insufficient detail to use Equation (3) directly. The reported $\delta D^\times_{gb,O}$ values were therefore multiplied by 1/6 $\Delta\ln p(O_2)$ as discussed for Ti_3AlC_2. Shown as the red stars in Figures 1 and 2, reasonably good agreement with the FeCrAl(Zr) baseline is observed, except perhaps at 900 °C. The 48 h MA 956 data from (Messaoudi et al., 1998) (small red circles) yields perhaps the most divergence from the Arrhenius baseline, with no apparent explanation at present.

Precise relations for scale thickness and interfacial grain size were reported for MA 956 and Kanthal APM (ZrO_2-oxide dispersed FeCrAl) oxidized at 1200 °C for up to 300 h (Tolpygo, 2008) (Tolpygo, private communication). In that study, the scale thickness (x) and grain size (G) were described by the power law relations below. A, B are scale growth constants, m is the grain growth exponent, and k is a grain growth constant, as listed in Table 2:

$$x^2 = At + B\frac{G^m - G_o^m}{Gk(m-1)} \tag{13}$$

$$G = (G_o^m + kt)^{1/m} \tag{14}$$

It then follows that:

$$\Pi = AG_i + B/m \tag{15}$$

The corresponding $\delta D_{gb,O,int.}$, given as hexagons in Figures 2 and 3, are seen to be slightly above the FeCrAl(Zr) reference line in juxtaposition to some of the previous values below the line. Overall, reasonable consistency is seen for $\delta D_{gb,O,int.}$ determined for the various FeCrAl(X) alloys and in the same range as the MAX phase alloys.

TABLE 2.—TOLPYGO'S OXIDATION AND GRAIN GROWTH
CONSTANTS FOR KINETIC EQUATIONS (13) TO (15) (TOLPYGO, 2008)

	A, $\mu m^2/h$	B	G_0 μm	k	m
MA956	0.0455	2.5513	0.1755	0.0146	4.4693
APM	−0.0228	1.8455	0.3615	0.0161	3.4700

While a single value of Π is sufficient to warrant inclusion in the previous plots, a number of these studies followed kinetics and grain size over a substantial time interval. This allows the determination of multiple values of Π versus time at one temperature, which lead to highly validated average values of $\delta D_{gb,O,int.}$. Examples of the studies that provided detailed kinetic fits at 1200 °C, and thus Π versus t, are provided in Figure 4 (Tallman et al., 2013) (Tolpygo, 2008) (Naumenko et al., 2007)(Smialek et al., 2013). The FeCrAl(Zr) behavior had been presented for 1100 to 1400 °C in a more compressed plot (Smialek et al., 2013). Much of the data indicated periods of nearly constant values, as expected for scale growth controlled by a constant value of $\delta D_{gb,O,int.}$ for a given temperature. This is especially born out for the 2000 h FeCrAlY and 2800 h Ti$_2$AlC results (Naumenko et al., 2007) (Tallman et al., 2013).

It is significant that this treatment produced a self-consistent assessment of data from 12 studies on 15 materials. There is no consistent or dramatic difference between scales doped with Ti, Zr, or Y, with perhaps the largest reduction (3x) shown by Y-doping (B. Pint, 1992). Given that all the validated data falls within tight bands shown in Figure 2, it can be expected that variation limits for the activation energy may be so defined. It is found that these bands define a slope, with $Q \approx 375 \pm 25$ kJ/mole, which can be taken as a working value for the nearly invariant primary rate controlling factor for oxidation, i.e., inward oxygen grain boundary diffusion. It is subject to assumptions of minimal contributions from Al diffusion. Slight variability may also be expected from different oxidation environments, such as dry or humid Ar-O$_2$, N$_2$-O$_2$, or pure O$_2$, which are not differentiated or addressed here. It is nevertheless more fundamental than activation energies obtained from the oxidation constant alone, now widely accepted to be affected by an indeterminate grain growth process and its temperature dependence. Alternatively, more attention can be focused on the oxidation product, Π, as proposed for FeCrAl(Zr), as a more invariant constant (i.e., equivalent to '2C' in (Naumenko et al., 2007).
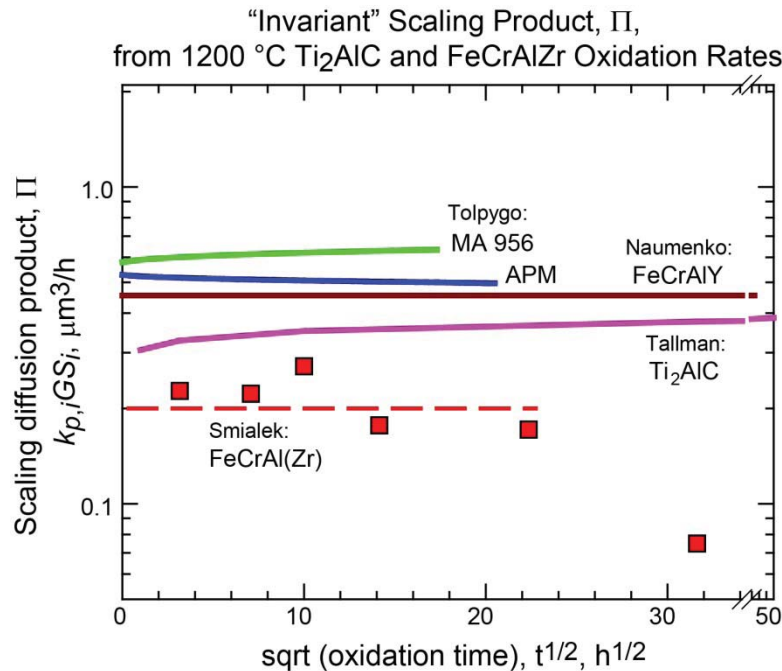

Figure 4.—Time invariant oxidation product, Π, at 1200 °C for Ti$_2$AlC MAX phase and four FeCrAl(X) alloys.

These $\delta D_{gb,O,int.}$ and activation energy enable more direct comparisons to diffusivity measured for bulk alumina. The oxidation analysis produced diffusivities 10 to 40x lower than those predicted from bulk alumina permeability studies, with an activation energy of 375 kJ/mole compared to 300 kJ/mole (Wada et al., 2011) (Smialek et al., 2013), and already discussed at length without a totally satisfactory resolution. Dopant effects and atomistic models of transport explain some of the discrepancy and provide deeper insight into mechanisms (Matsudaira, Wada, Saitoh, and Kitaoka, 2010) (Matsudaira, Wada, Saitoh, and Kitaoka, 2011) (Matsudaira, Wada, and Kitaoka, 2013) (Heuer, Hovis, Smialek, and Gleeson, 2011) (Heuer et al., 2013). Some aluminum outward diffusion is well-documented, but is considered to be less important since oxygen inward diffusion predominates through the majority of the scale (Wada et al., 2011). These topics warrant further discussion, but at present cannot resolve all discrepancies and are considered beyond the scope of this paper.

It should be pointed out that the $\Pi/12$ solution was enabled by assuming the $p(O_2)^{-1/6}$ dependency of oxygen diffusion as verified by (Wada et al., 2011) and Equation (1). However its possible role, associated with $V_O^{\bullet\bullet}$ creation predicted from classic Kroger-Vink equilibrium and charge neutrality conditions, has indeed been raised a number of times, for example by (Ramanarayanan et al., 1984) (Pint, 1992) (Pint and Deacon, 2005) (Messaoudi et al., 1998). The solution from Pint et al. also highlighted the dominant $p(O_2)_{int.}$ aspect of controlling inward oxygen diffusion as compared to the external pressure, leading to a concise working relation such as Equation (3). This can be further addressed by the appropriate $p(O_2)_{eq}$ correction (Eq. (6)) to give a more general relation for other $p(O_2)$ along the format of Pint and Equation (1):

$$\delta D_{gb,O} = 7.567 \times 10^{-8} \exp\left(\frac{-544\,\text{kJ}}{RT}\right) p_{O_2}^{-1/6} \frac{\text{m}^3}{\text{s} \cdot \text{Pa}^{-1/6}} \tag{16}$$

This equation is useful for comparisons to tracer studies in bulk alumina under atmospheric conditions, which indicate reductions of 10^2 to 10^5 when compared to alumina scale transport.

Summary

Published oxidation data for Ti_3AlC_2, Ti_2AlC, and Cr_2AlC have been analyzed by a recent modification of the Wagner solution by which the oxidation product $\Pi = 12\delta D_{gb,O,int.}$. The values so determined were found to be in the same population as numerous similar studies of FeCrAl(X) oxidation. Neither group showed any large or consistent trend with either Cr, Ti, Zr, Y, ZrO_2, or Y_2O_3 doping. Thus most behaviors are adequately generally described by the relation developed for FeCrAl(Zr):

$$\delta D_{gb,O,int} = 1.8 \times 10^{-10} \exp\left(\frac{-375\,\text{kJ}}{RT}\right) \text{m}^3/\text{s} \tag{4}$$

Oxidation results were shown for just one value for Π as well as multiple detailed measurements, sometimes spanning thousands of hours at a given temperature. Studies assuming a constant diffusion product, $\delta D^{\times}_{gb,O}$, were adjusted by the factor $1/6\ \Delta\ln[p(O_2)]$. This produced values consistent with the present Wagner solution where $\delta D_{gb,O}$ was assumed to vary as $p(O_2)^{-1/6}$. In summation, a large population of alumina scale kinetic data, normalized by grain size and spanning 900 to 1400 °C, cluster about a single relation based on oxygen grain boundary diffusion control.

References

Bale, C.W., Bélisle, E., Chartrand, P., Decterov, S.A., Eriksson, G., Hack, K., … Petersen, S. (2009). FactSage thermochemical software and databases---recent developments. *Calphad*, *33*, 295–311. doi:10.1016/j.calphad.2008.09.009

Barsoum, M.W., and El-raghy, T. (2001). The MAX Phases: Unique New Carbide and Nitride Materials. *American Scientist*, *89*(July-August), 334–343.

Chen, S.L., Daniel, S., Zhang, F., Chang, Y.A., Yan, X.Y., Xie, F.Y., … Oates, W.A. (2002). The PANDAT software package and its applications. *Calphad: Computer Coupling of Phase Diagrams and Thermochemistry*, *26*, 175–188. doi:10.1016/S0364-5916(02)00034-2

Clemens, D., Bongartz, K., Quadakkers, W.J., Nickel, H., Holzbrecher, H., and Becker, J.S. (1995). Determination of lattice and grain boundary diffusion coefficients in protective alumina scales on high temperature alloys using SEM, TEM and SIMS. *Analytical and Bioanalytical Chemistry*, *353*(3-4), 267–70. doi:10.1007/s0021653530267

Hajas, D. E., to Baben, M., Hallstedt, B., Iskandar, R., Mayer, J., & Schneider, J. M. (2011). Oxidation of Cr2AlC coatings in the temperature range of 1230 to 1410°C. *Surface and Coatings Technology*, *206*(4), 591–598. doi:10.1016/j.surfcoat.2011.03.086

Heuer, A.H., Hovis, D.B., Smialek, J.L., and Gleeson, B. (2011). Alumina Scale Formation: A New Perspective. *Journal of the American Ceramic Society*, *94*, s146–s153. doi:10.1111/j.1551-2916.2011.04573.x

Heuer, A.H., Nakagawa, T., Azar, M.Z., Hovis, D.B., Smialek, J.L., Gleeson, B., … Finnis, M.W. (2013). On the growth of Al_2O_3 scales. *Acta Materialia*, *61*(18), 6670–6683. doi:10.1016/j.actamat.2013.07.024

Lee, D.B., and Park, S.W. (2007). Oxidation of Cr_2AlC Between 900 and 1200 °C in Air. *Oxidation of Metals*, *68*(5-6), 211–222. doi:10.1007/s11085-007-9071-0

Matsudaira, T., Wada, M., and Kitaoka, S. (2013). Effect of Dopants on the Distribution of Aluminum and Oxygen Fluxes in Polycrystalline Alumina Under Oxygen Potential Gradients at High Temperatures. *Journal of the American Ceramic Society*, *9*, 1–9. doi:10.1111/jace.12420

Matsudaira, T., Wada, M., Saitoh, T., and Kitaoka, S. (2010). The effect of lutetium dopant on oxygen permeability of alumina polycrystals under oxygen potential gradients at ultra-high temperatures. *Acta Materialia*, *58*(5), 1544–1553. doi:10.1016/j.actamat.2009.10.062

Matsudaira, T., Wada, M., Saitoh, T., and Kitaoka, S. (2011). Oxygen permeability in cation-doped polycrystalline alumina under oxygen potential gradients at high temperatures. *Acta Materialia*, *59*(14), 5440–5450. doi:10.1016/j.actamat.2011.05.018

Messaoudi, K., Huntz, A., and Lesage, B. (1998). Diffusion and growth mechanism of Al_2O_3 scales on ferritic Fe-Cr-Al alloys. *Materials Science and Engineering: A*, *247*(1-2), 248–262. doi:10.1016/S0921-5093(97)00711-9

Naumenko, D., Gleeson, B., Wessel, E., Singheiser, L., and Quadakkers, W.J. (2007). Correlation between the Microstructure, Growth Mechanism, and Growth Kinetics of Alumina Scales on a FeCrAlY Alloy. *Metallurgical and Materials Transactions A*, *38*(12), 2974–2983. doi:10.1007/s11661-007-9342-z

Pint, B. (1992). The Effect of Reactive Elements on the Growth of Al_2O_3 Scales. Massachusets Institute of Technology.

Pint, B.A., and Deacon, R.M. (2005). Comment on "Oxidation of alloys containing aluminum and diffusion in Al_2O_3" [J. Appl. Phys. 95, 3217 (2004)]. *Journal of Applied Physics*, *97*(11), 116111. doi:10.1063/1.1923610

Ramanarayanan, T.A., Raghavan, M., and Petkovic-Luton. (1984). The Characteristics of Alumina Scales Formed on Fe-Based Yttria- Dispersed Alloys. *J. Electrochemical Society*, *131*(4), 923–931.

Smialek, J.L. and Garg, A. (2014). *Microstructure and Oxidation of a MAX Phase/Superalloy Hybrid Interface*, NASA/TM—2014-216679, Cleveland.

Smialek, J.L., Jacobson, N.S., Gleeson, B., Hovis, D.B., and Heuer, A.H. (2013). Oxygen Permeability and Grain-Boundary Diffusion Applied to Alumina Scales. NASA/TM—2013-217855, 1–14.

Song, G.M., Schnabel, V., Kwakernaak, C., van der Zwaag, S., Schneider, J.M., and Sloof, W.G. (2012). High temperature oxidation behaviour of Ti_2AlC ceramic at 1200°C. *Materials at High Temperatures*, *29*(3), 205–209. doi:10.3184/096034012X13348496462140

Tallman, D.J., Anasori, B., and Barsoum, M.W. (2013). A Critical Review of the Oxidation of Ti_2AlC, Ti_3AlC_2 and Cr_2AlC in Air. *Materials Research Letters*, *1*(3), 115–125. doi:10.1080/21663831.2013.806364

Tolpygo, V. (2008). Grain coarsening in alumina scales and its effect on the oxidation kinetics of Fe-Cr-Al alloys. In *High Temperature Corrosion and Protection of Materials* (presentation at HTCPM, 2008, les Embiez). doi:10.1016/B978-0-08-013342-3.50005-9

Wada, M., Matsudaira, T., and Kitaoka, S. (2011). Mutual grain-boundary transport of aluminum and oxygen in polycrystalline Al_2O_3 under oxygen potential gradients at high temperatures. *J. Ceram. Soc. Jpn*, *119*(11), 832–839. Retrieved from http://people.virginia.edu/~lz2n/mse6020/articles/Wada-JCSJ11.pdf

Wang, L., Chen, Z., Ti_3AlC_2 oxidation mechanism, Corrosion Science 58 (2012) 95–103

Wang, X.H., and Zhou, Y.C. (2003a). High-Temperature Oxidation Behavior of Ti_2AlC in Air. *Oxidation of Metals*, *59*(April), 303–320.

Wang, X.H., and Zhou, Y.C. (2003b). Oxidation behavior of Ti_3AlC_2 at 1000-1400 °C in air. *Corrosion Science*, *45*, 891–907. doi:10.1016/S0010-938X(02)00177-4

Wang, X.H., Li, F.Z., Chen, J.X., and Zhou, Y.C. (2012). Insights into high temperature oxidation of Al_2O_3-forming Ti_3AlC_2. *Corrosion Science*, *58*, 95–103. doi:10.1016/j.corsci.2012.01.011

Young, D.J., Naumenko, D., Niewolak, L., Wessel, E., Singheiser, L., and Quadakkers, W.J. (2010). Oxidation kinetics of Y-doped FeCrAl-alloys in low and high pO_2 gases. *Materials and Corrosion*, *61*(10), 838–844. doi:10.1002/maco.200905432